

PRESSURE-SUPPORTED IONIZED GAS IN S0 GALAXIES¹

FRANCESCO BERTOLA, PIERATONIO CINZANO, ENRICO MARIA CORSINI
 Dipartimento di Astronomia, Università di Padova, vicolo dell'Osservatorio 5, I-35122 Padova, Italy

HANS-WALTER RIX
 Max-Planck-Institut für Astrophysik, Karl Schwarzschild Straße 1, D-85748 Garching bei München, Germany

AND

WERNER W. ZEILINGER
 Institut für Astronomie, Universität Wien, Türkenschanzstraße 17, A-1180 Wien, Austria
Received 1995 April 11; accepted 1995 May 10

ABSTRACT

Rotation curves and velocity dispersion profiles are presented for both the stellar and gaseous components of a sample of S0 galaxies. In all galaxies the central velocity dispersion of the ionized gas exceeds 150 km s^{-1} . In some galaxies the gas dispersion remains as high as the stellar one over an extended radial range, showing that random motions are crucial for the dynamical support of the gas. Such a pressure support may explain why the observed gas rotation curves in galaxy bulges often fall short of the circular velocity predicted from the stellar kinematic models. It is suggested that, in addition to the acquisition of external material, some of the observed gas in S0 galaxies may have been shed from bulge stars.

Subject headings: galaxies: elliptical and lenticular, cD — galaxies: kinematics and dynamics — galaxies: structure

1. INTRODUCTION

It has been argued (Bertola, Buson, & Zeilinger 1992) that the frequent cases of S0 galaxies where gas is found in counterrotation with respect to the stellar component indicate that the ionized gas is often of external origin. A detailed kinematic analysis of eight S0 galaxies, presented in this Letter, has led to the detection of an additional gaseous component of high-velocity dispersion. Several observational results hinted in the past at the presence of such a component. Fillmore, Boroson, & Dressler (1986), studying a sample of moderately inclined spiral galaxies, discovered that the inner portion of the gas rotation curve systematically falls below the circular velocities predicted by models using the stellar rotation and velocity dispersion curves. Similarly, Kent (1988) found in a sample of Sa galaxies that the inner $\text{H}\alpha$ rotation curves often fall short of the circular velocities predicted by constant M/L models, normalized at large radii. Both authors suspected that this discrepancy arises because the ionized gas is not in a cold disk at small radii but in some way is associated with the bulge stars. Such gas could either be shed by bulge stars or be connected to X-ray halo. If correct, the gas may be largely supported by noncircular random motions (i.e., velocity dispersion) and therefore may be rotating at much less than the circular velocity. Such high-velocity dispersions for the ionized gas have been observed in the nuclei of elliptical galaxies (e.g., Bertola et al. 1984).

To explain the discrepancy between the observed gas rotation and the predicted circular velocity and to address the origin of the gas, we need a crucial piece of information, which has been missing so far: the radial trend of the gas velocity dispersion. The main purpose of this Letter is to present such data and use them to address the above issues.

2. SAMPLE AND OBSERVATIONS

The sample of eight S0 galaxies (see Table 1) was selected to have known extended gas emission. The rotation curves for two of the galaxies, found to exhibit gas-star counterrotation, were presented earlier (Bertola et al. 1992).

All observations were carried out with the Red Channel Spectrograph at the MMT using a $1200 \text{ grooves mm}^{-1}$ grating and a Texas Instrument CCD with 800×800 pixels ($15 \times 15 \mu\text{m}^2$ pixel size). The slit was set along the major axis of the galaxies (see Table 1). At a dispersion of $0.82 \text{ \AA pixel}^{-1}$ the spectra ranged from 3650 \AA to 4300 \AA , including the Ca II H and K stellar lines, the G-band, and the [O II] gas emission doublet at $3726.2\text{--}3728.9 \text{ \AA}$. With a slit width of $1''.25$ the instrumental resolution was $\sigma = 1.1 \text{ \AA}$, i.e., approximately 83 km s^{-1} at 3975 \AA and approximately 88 km s^{-1} at 3727 \AA . The spatial scale perpendicular to the dispersion was $0''.33 \text{ pixel}^{-1}$ yielding a field of about $3'$. No binning or rebinning was done. The seeing during the observations ranged from $1''$ to $1''.5$ FWHM. The exposure time per object was 60 minutes. Spectra of nonrotating giant stars with types ranging from late G to early K were obtained with the same instrumental setup for use as velocity and dispersion templates. The spectra were reduced and calibrated in the same way as described by (Bertola et al. 1988). Sky subtraction was done using the available data at the ends of the slit.

The stellar kinematics were analyzed with the Fourier Quotient Method (Sargent et al. 1977) as applied by (Bertola et al. 1984) with the spectra rebinned to yield constant signal-to-noise ratio (S/N).

The [O II] emission doublet was not resolved in the MMT spectra for any of the objects. Therefore, it was analyzed by fitting a double Gaussian to the line profile, fixing the ratio between the intensities of the two lines, fixing the ratio between the two wavelengths, and assuming that both lines have the same dispersion. The intensity ratio was judged by

¹ The observations reported here were obtained with the Multiple Mirror Telescope, a joint facility of the University of Arizona and the Smithsonian Institution.

TABLE 1
OBSERVED GALAXIES

Object	Type ^a	Scale ^a (arcsec pc ⁻¹)	<i>b/a</i> ^b	P.A. ^c	<i>m_B</i> ^b	<i>V_{sys}</i> ^c (km s ⁻¹)
NGC 2768	S0 _{1/2} (6)	0.37	0.52	90°	10.76	1400
NGC 2787	SB0/a	0.71	0.65	117°	11.84	723
NGC 3414	S0 _{1/2} (0)/a	0.43	0.72	35°	11.82	1480
NGC 3489	S0 ₃ /Sa	1.11	0.58	30°	11.30	770
NGC 3945	RSB0 ₂	0.44	0.66	145°	11.40	1250
NGC 4036	S0 ₃ (8)/Sa	0.39	0.40	85°	11.55	1420
NGC 4111	S0 ₁ (9)	0.72	0.21	149°	11.63	790
NGC 4379	S0 _{1/2} (2)	0.64	0.85	105°	12.63	1070

^a From Sandage & Tamman 1987.

^b From de Vaucouleurs et al. 1991.

^c This paper.

eye for each galaxy from the shape of the line profile. Owing to the faint level, the emission lines of 4379 were instead fitted with a single Gaussian.

3. RESULTS

The resulting kinematics for all eight sample members is summarized in Figure 1. All rotation values shown are as

observed; no inclination correction has been applied. Here we discuss briefly each individual object.

1. *NGC 2768*.—The stars in the bulge show very little rotation ($v/\sigma \approx 0.2$). The gas is apparently in counterrotation (Bertola et al. 1992) and has a maximum rotation velocity of 60 km s⁻¹. The gas velocity dispersion reaches 200 km s⁻¹ at the center but drops rapidly to very low values. In contrast, the stellar velocity dispersion remains high ($\sigma_{\text{stars}} > 200$ km s⁻¹), possibly even rising away from the nucleus.

2. *NGC 2787*.—The gas velocity dispersion peaks at 150 km s⁻¹ but falls rapidly to values of $\sigma_{\text{gas}} \approx 50$ km s⁻¹. From 2" to about 10" the gas kinematics is dominated by rotation. The central velocity gradient in the gas is equal to that of the stars.

3. *NGC 3414*.—The gas velocity curve of this edge-on galaxy has a steep gradient, reaching 140 km s⁻¹ at 2" from the center. The gas dispersion is low outside 2" but strongly peaked in the center. This central peak may be partly due to the seeing smearing of the rotating curve. The stars rotate much more slowly with a maximum velocity less than 40 km s⁻¹ (compared to the central velocity dispersion of $\sigma_{\text{stars}} \approx 250$ km s⁻¹). Note that the stellar dispersion shows a strong drop beyond 7".

4. *NGC 3489*.—Except for the inner 1", the gas velocity

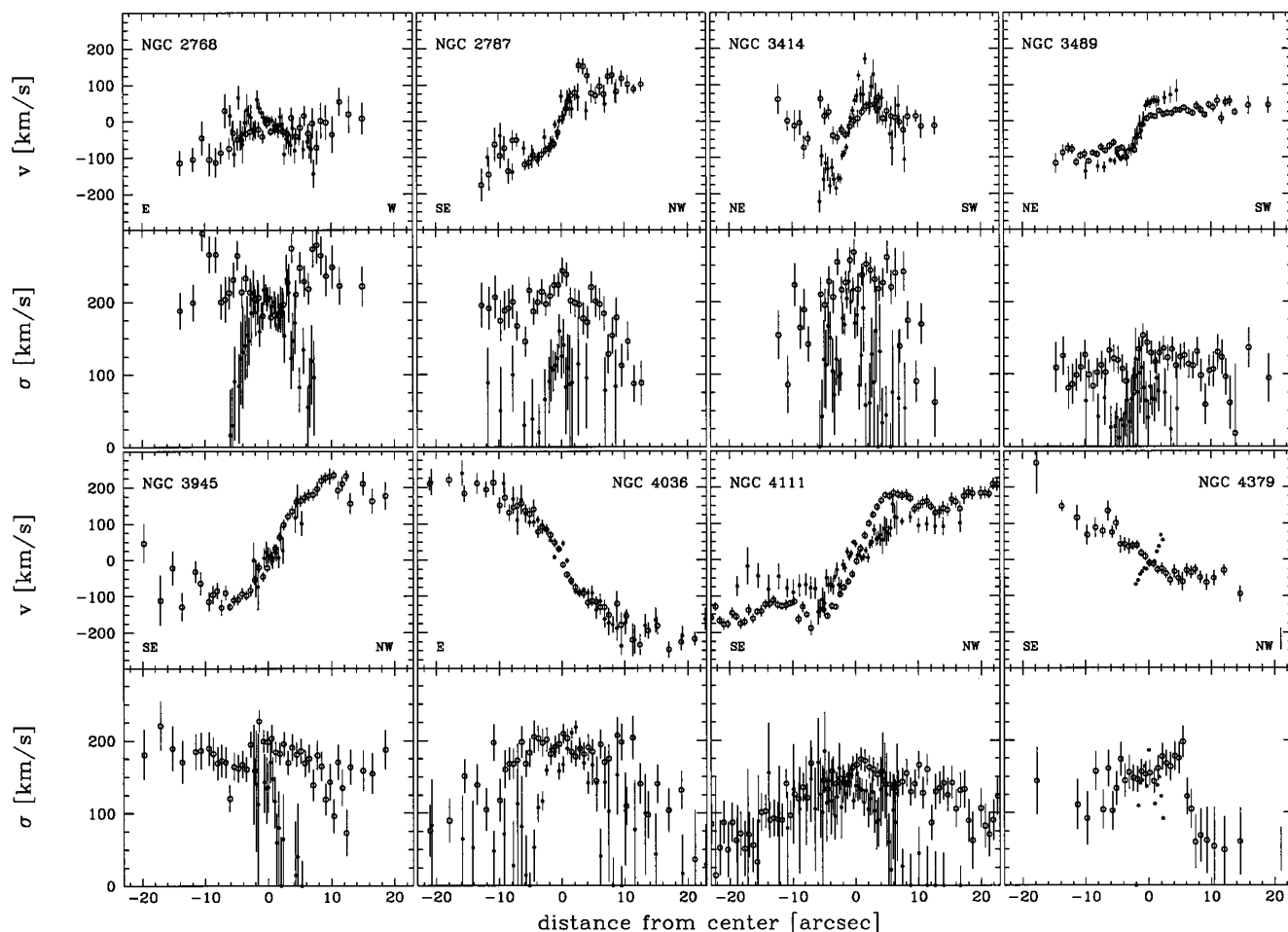


FIG. 1.—Rotation and velocity dispersion curves for the stars (*open circles*) and the ionized gas (*filled circles*) in NGC 2768, NGC 2787, NGC 3414, NGC 3489, NGC 3945, NGC 4036, NGC 4111, and NGC 4379. The systemic line-of-sight velocities for all the objects are in Table 1. The gas error bars indicate the formal error of double Gaussian fit. The errors on the gas velocity dispersion also account for the subtraction of the instrumental dispersion. In the case of NGC 4379, whose emission lines were fitted with a single Gaussian, the bar on the right-hand side of each panel represents the typical measurement error for the gas.

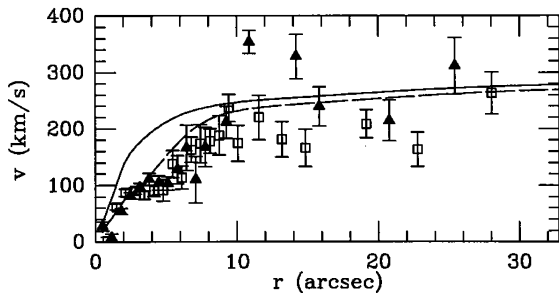


FIG. 2.—Comparison of the observed gas rotation velocity in NGC 4036 with (a) the true circular velocity (solid line), derived from the stellar kinematics and (b) the rotation speed (dashed line) predicted by a kinematic model which takes proper account of the gas velocity dispersion (Cinzano et al. 1995).

dispersion is low ($\sigma_{\text{gas}} \approx 50 \text{ km s}^{-1}$), indicating that the gas is predominantly supported by rotation. The central velocity gradient of the gas is somewhat steeper than that of the stars.

5. *NGC 3945*.—The emission-line kinematics can only be measured within $3''$. The dispersion seems to drop rapidly from a central value of 150 km s^{-1} .

6. *NGC 4036*.—Inside $5''$ the gas dispersion in this galaxy shows a plateau at a value of $\approx 180 \text{ km s}^{-1}$. At larger radii the dispersion drops to low values. The gas rotation increases linearly with distance from the galaxy center out to $12''$ and tracks the stellar rotation remarkably well. Qualitatively, these data indicate that the gas is pressure supported inside $5''$ and rotation supported beyond. The gas and star data on this galaxy are of sufficient quality to permit the construction of detailed kinematic models, trying to explain the gas and star kinematics, assuming they both orbit in the potential provided by the stars. These models (Cinzano et al. 1995) show, allowing for the gas dispersion, how the gas rotation may fall far short of the circular velocity (Fig. 2).

7. *NGC 4111*.—Similar to NGC 4036, the gas dispersion remains high ($\sigma_{\text{gas}} \geq 100 \text{ km s}^{-1}$) for $R < 5''$. In this region the gas appears to be pressure supported. It is unclear how rapidly the gas dispersion drops beyond these radii. The gas rotation ($v_{\text{gas}} \leq 100 \text{ km s}^{-1}$), on the other hand, is much lower than naively expected from the stellar kinematics ($v_{\text{stars}} \approx 150 \text{ km s}^{-1}$).

8. *NGC 4379*.—This galaxy is the second example of star-gas counterrotation. The gas exhibits a steeper rotation gradient than the stars but cannot be traced to the turnover of the rotation curve. The detectable gas is confined to the inner $4''$. The gas velocity dispersion shows a narrow peak within this region.

For detailed modeling of the gas kinematics, data along other position angles would be very important. Any model based solely on major axis spectra must rely on the uncertain assumption that the gas distribution is aligned with the plane of the stellar disk.

4. DISCUSSION AND CONCLUSIONS

The rotation and velocity dispersion curves for the gas and the stars in the S0 galaxies presented here reveal a complex phenomenology. The following kinematic features are note-

worthy: there are sample galaxies in which the central velocity gradient of the ionized gas is steeper (NGC 2768, NGC 3414, NGC 3489), equal to (NGC 2787, NGC 3945, NGC 4036, NGC 4379), shallower (NGC 4111) than the stellar velocity gradient. Only the first case would be expected if the gas traced the local circular velocity. In all cases the observed central velocity dispersion rises to values above 100 km s^{-1} . In a good number of cases, in particular the cases of steep velocity gradients (NGC 3414, NGC 4379), the dispersion drops rapidly outward, and the gas becomes rotation dominated. In at least two cases (NGC 4036, NGC 4111) the gas dispersion remains high ($\sigma_{\text{gas}} > 100 \text{ km s}^{-1}$) for all radii $< 5''$. In these cases it is very clear that the seeing smearing of velocity gradients plays little role.

A detailed modeling of the stellar and gaseous kinematics for NGC 4036 (Cinzano et al. 1995; see also the model for NGC 2974, Cinzano & van der Marel 1994) shows that the difference between the true *circular velocity*, inferred from modeling of the stellar kinematics, and the observed gas rotation speed can be explained when accounting for the velocity dispersion of the gas (see Fig. 2). Such models, together with the frequency of high-velocity dispersion gas, may provide a natural explanation for the “too slowly” rising gas rotation curves, inferred previously under the assumption that the gas rotation traces the circular velocity (Fillmore et al. 1986; Kent 1988; Kormendy & Westpfahl 1989).

The manifest presence of dynamically hot gas (i.e., with a projected velocity dispersion comparable to its rotation) naturally leads to the question of its origin. A plausible explanation, discussed previously by various authors (Bertola et al. 1984; Fillmore et al. 1986; Kent 1988; Kormendy & Westpfahl 1989), is that some of the ionized gas found in these bulges constitutes material recently lost from the stars but not yet heated to the virial temperature of the galaxy. Simple estimates (e.g., Bertola et al. 1984) for elliptical galaxies, scaled to the lower masses of S0 bulges, show that there is enough gas shed from the stars to produce the observed emission lines of high-velocity dispersion. The UV rising branch in the spectral energy distribution of the bulges (Burstein et al. 1988) produced by evolved stars (Bertola et al. 1995) can be the source of ionizing radiation producing the emission lines (Di Serego Alighieri et al. 1990). Such an origin of the gas may also explain the conspicuous coincidence of the gas and stellar rotation curves as observed, e.g., in NGC 4036.

Finally, we should note that the gas shed from stars will of course always be in corotation with the stars. If the gas in S0 galaxies in emission lines partly comes from internal sources (mass loss) and partly comes from infall at random angles, one would expect that corotating gas is somewhat more frequent than counterrotating gas, as observed (Bertola et al. 1992).

W.W.Z. acknowledges the support of the Austrian Fonds zur Förderung der wissenschaftlichen Forschung (project J00934-PHY).

REFERENCES

- Bertola, F., Bettoni, D., Rusconi, L., & Sedmak, G. 1984, *AJ*, 89, 356
 Bertola, F., Bressan, A., Burstein, D., Buson, L. M., Chiosi, C., & di Serego Alighieri, S. 1995, *ApJ*, 438, 680
 Bertola, F., Buson, L. M., & Zeilinger, W. W. 1992, *ApJ*, 401, L79
 Bertola, F., Galletta, G., Kotanyi, C., & Zeilinger, W. W. 1988, *MNRAS*, 234, 733
 Burstein, D., Bertola, F., Buson, L. M., Faber, S. M., & Lauer, T. R. 1988, *ApJ*, 328, 440
 Cinzano, P., Rix, H.-W., Zeilinger, W. W., & Bertola, F. 1995, in preparation
 Cinzano, P., & van der Marel, R. P. 1994, *MNRAS*, 270, 325
 de Vaucouleurs, G., de Vaucouleurs, A., Corwin, H. G., Jr., Buta, R. J., Paturel,

- H. G., & Fouqué, P. 1991, 3d Reference Catalogue of Bright Galaxies (New York: Springer)
- Di Serego Alighieri, S., Trinchieri, G., & Brocato, E. 1990, in Windows on Galaxies, ed. G. Fabbiano, J. Gallagher, & A. Renzini (Dordrecht: Kluwer), 301
- Fillmore, J. A., Boroson, T. A., & Dressler, A. 1986, ApJ, 302, 208
- Kent, S. M. 1988, AJ, 96, 514
- Kormendy, J., & Westpfahl, D. J. 1989, ApJ, 338, 752
- Sandage, A., & Tamman, G. A. 1987, A Revised Shapley-Ames Catalog of Bright Galaxies (Washington: Carnegie Inst.)
- Sargent, W. L. W., Schechter, P. L., Boksenberg, A., & Shortridge, K. 1977, ApJ, 212, 326